

## Propagation of a Rippled Shock Wave Driven by Nonuniform Laser Ablation

R. Ishizaki and K. Nishihara

*Institute of Laser Engineering, Osaka University, 2-6 Yamada-oka, Suita, Osaka 565, Japan*

(Received 16 August 1996)

A simple analytical model is presented to study hydrodynamic perturbation growth in the start-up phase in laser fusion, namely propagation of a rippled shock driven by nonuniform laser ablation induced by initial target roughness or nonuniform laser irradiation. Analytical results agree quite well with experimental data for the rippled shock propagation in the case of uniform irradiation on a rough surface. Approximate formulas expressing both the time evolution of the shock front and the asymptotic behavior of the ablation front are obtained in the weak shock limit. [S0031-9007(97)02627-6]

PACS numbers: 52.35.Tc, 52.35.Py, 52.50.Jm

To achieve ignition and high gain in inertial confinement fusion (ICF) [1], a spherical pellet must implode efficiently and symmetrically. A shock wave driven by the laser ablation propagates through a shell, and shell acceleration then follows. Hydrodynamic perturbation growth in the shock-compressed phase seeds the Rayleigh-Taylor (RT) instability [2,3] in the subsequent acceleration. The study of the hydrodynamic perturbation growth is thus essential for a better understanding of the RT instability that is important not only in ICF but also in supernova explosions [4].

When ablation pressure is applied on a target with a rippled surface, a rippled shock wave is launched in accordance with the target surface. Also, when a uniform target is nonuniformly irradiated by a laser beam, a rippled shock is driven by nonuniform ablation pressure. The oscillation of the rippled shock would generate hydrodynamic perturbations [5]. In this paper, a simple analytical model is developed to study propagation of a rippled shock associated with an initial surface roughness of a target and nonuniform laser irradiation on a smooth target. It will be shown that the temporal evolution of the rippled shock front and the deformation of the ablation surface can be obtained by solving a linear wave equation in the shock-compressed region with suitable boundary conditions, for example, the Rankine-Hugoniot (RH) jump condition at the shock front [6–9], and the Chapman-Jouguet deflagration (CJ) jump condition at the laser ablation surface [10]. We show explicit analytical solutions of the model equation, and obtain approximate formulas in the weak shock limit [11]. Some of the solutions are compared with recent experimental results [5]. It should be mentioned that since the model is based on the linear theory and the assumption of a stationary laser ablation as the zeroth order hydrodynamics, the theory may be difficult to be applied directly to imprint experiments [12]. In those experiments, a significant imprint may be created by nonuniform laser irradiation before the stationary laser ablation takes place. Despite this fact, analytical solutions are useful to understand the underlying physics and the dependence on laser and target parameters.

At first, we sketch briefly the zeroth order profiles of a stationary shock wave driven by a steady laser ablation. The domain can be separated into four regions by the shock front, ablation front, and sonic point as shown in Fig. 1. We label these regions 0, 1, A, and 2 from right to left. The region 0 is a uniform state ahead of the shock, the region 1 is the shock-compressed region, the region A is an ablation region between the ablation front and the sonic point, and the region 2 beyond the sonic point is an isothermal rarefaction region. We can apply the RH jump conditions at the shock front:

$$\frac{u_s}{V_0} = \frac{u_s - v_{x1}}{V_1} = \sqrt{\frac{p_1 - p_0}{V_0 - V_1}}, \quad (1a)$$

$$(\nu_0 V_0 - V_1)p_0 - (\nu_1 V_1 - V_0)p_1 = 0, \quad (1b)$$

and the CJ jump conditions at the ablation front:

$$\frac{u_a - v_{x1}}{V_1} = \frac{u_a - v_{x2}}{V_2} = \sqrt{\frac{p_2 - p_1}{V_1 - V_2}} = \dot{m} = \rho_1 v_a, \quad (2a)$$

$$(\nu_1 V_1 - V_2)p_1 - (\nu_2 V_2 - V_1)p_2 = -\frac{2I}{\dot{m}}, \quad (2b)$$

where  $u_s$ ,  $u_a$ , and  $v_x$  are the shock and ablation surface velocities and fluid velocity in a laboratory frame, and

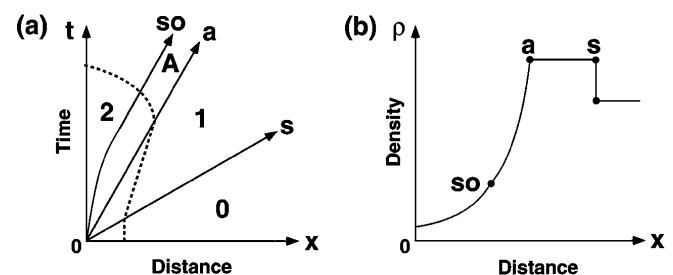


FIG. 1. Schematic diagram of shock propagation driven by laser ablation: (a)  $x-t$  diagram, and (b) density profile at certain time.  $s$ ,  $a$ , and  $so$  denote shock front, ablation front, and sonic point, respectively. 0, 1, A, and 2 denote unperturbed, shock compressed, deflagration, and isothermal rarefaction regions, respectively. Dashed line in (a) shows fluid flow.

$p$ ,  $\rho$ , and  $V$  are pressure, density, and specific volume, respectively.  $v_a$  is the ablation velocity in a reference frame moving with the fluid in the compression region.  $\dot{m}$  and  $I$  are the mass ablation rate and absorbed laser intensity, respectively, and  $\nu = (\gamma + 1)/(\gamma - 1)$  and  $\gamma$  is isentropic exponent. The subscripts 0, 1, and 2 denote the values of the regions 0, 1, and 2, respectively. The fluid velocity of the sonic point relative to the ablation surface is equal to the sound speed of the sonic point,  $u_a - v_{x2} = \sqrt{p_2 V_2}$ . We can uniquely determine the zeroth order variables in each region by using these conditions, once the uniform state ahead of the shock ( $p_0, V_0$ ) and the absorbed laser intensity and the density at the sonic point ( $I, V_2$ ) are given. We assume the density of the sonic point is the laser cut-off density [13]. The sonic point density may not always be the cut-off density especially for short wavelength lasers. However, this assumption is not so inaccurate in the case that low- $Z$  target is irradiated by 0.53  $\mu\text{m}$  laser. For a shorter wavelength laser, we can solve the zeroth order jump conditions by using the observed ablation pressure ( $p_1$ ) or mass ablation rate ( $\dot{m}$ ).

We consider a rippled shock wave and a nonuniform laser ablation caused by an initial surface roughness of a target or nonuniform laser irradiation on a smooth target. We assume the surface modulation of the target to be given as  $a_0 \exp(iky)$  in the former, and the nonuniform laser irradiation to be given as  $\delta I \exp(iky)$  in the latter, where  $a_0$ ,  $\delta I$ , and  $k$  are the surface amplitude, the perturbation of the absorbed laser intensity, and the perturbation wave number, respectively. These nonuniformities induce perturbations in the regions 1, A, and 2. According to the linear theory [6–9,11], the pressure perturbation in the shock-compressed region satisfies the wave equation in a reference frame moving with the fluid:

$$\frac{\partial^2}{\partial t'^2} \delta p_1(x', t') = c_1^2 \frac{\partial^2}{\partial t'^2} \delta p_1(x', t') - c_1^2 k^2 \delta p_1(x', t'), \quad (3)$$

where  $c_1$  is the sound speed and  $\delta p_1$  is perturbed pressure, and  $x' = x - v_{x1}t$  and  $t' = t$ . We can write the general solution of Eq. (3) as:

$$\delta p_1 = \sum_{\mu} (A_{\mu} e^{-\mu\theta} + B_{\mu} e^{-\mu\theta}) [C_{\mu} J_{\mu}(r) + D_{\mu} N_{\mu}(r)], \quad (4)$$

where  $r = kc_1 t' \sqrt{1 - (x'/c_1 t')^2}$ ,  $\theta = \tanh^{-1}(x'/c_1 t')$ ,  $\mu$  is a separation constant, and  $J_{\mu}$  and  $N_{\mu}$  are the Bessel and Neumann functions, respectively [6,7,11]. The coefficients  $A$ ,  $B$ ,  $C$ , and  $D$  as well as the separation constant  $\mu$  must be determined by the boundary and initial conditions. It should be noted that because entropy waves propagate with the fluid, an entropy perturbation in this region ( $\delta s_1 \propto \delta p_1/p_1 + \gamma_1 \delta V_1/V_1$ ) does not depend on time in the reference frame moving with the fluid.

The boundary conditions at the shock front are the same as in previous works [6–9]. For instance, linearizing

Eq. (1a), the time derivative of the shock front ripple,  $\dot{a}_s$ , is given by:

$$\dot{a}_s(t) \equiv \delta u_s(t) = \frac{\gamma_1 + 1}{4\rho_0 c_0 M_s} \delta p_1(u_s t, t), \quad (5)$$

where  $M_s$  is the shock Mach number, and we assume  $\gamma_0 = \gamma_1$  hereafter. At the ablation surface, linearizing Eq. (2), we get three equations which give relations between the perturbations at the ablation front and those at the sonic point [14]. For instance, linearizing Eq. (2a), the time derivative of the ablation surface ripple,  $\dot{a}_a (\equiv \delta u_a)$ , is given by:

$$\begin{aligned} \frac{\dot{a}_a(t) - \delta v_{x1}(u_a t, t)}{v_a} \\ = \frac{1}{1 - \bar{M}} \left( \frac{\delta p_1(u_a t, t) - \delta p_2(t)}{p_1} \right. \\ \left. + \frac{\delta V_1(u_a t, t) - \bar{M} \delta V_2(t)}{V_1} \right), \quad (6) \end{aligned}$$

where we assume that the distance of the region A is very short compared with the perturbation wavelength,  $\lambda (= 2\pi/k)$ , and  $\bar{M} = \gamma_1 (v_a/c_1)^2$ .  $v_a/c_1$  represents the ablation Mach number, which is much smaller than unity in general. We assume that the first-order quantities at the sonic point satisfy the condition that the local Mach number is equal to unity:

$$\frac{\dot{a}_a(t) - \delta v_{x2}(t)}{c_2} = \frac{1}{2} \left( \frac{\delta p_2(t)}{p_2} + \frac{\delta V_2(t)}{V_2} \right). \quad (7)$$

In addition, we make  $\delta V_2 \equiv 0$  because the density of the sonic point is taken to be the laser cut-off density [13]. It is noted that we are not solving the perturbation in region 2. Rather, we substitute that physics with Eq. (7) and the assumption that  $\delta V_2 \equiv 0$  at the sonic point. This could, in principle, be done because the flow in region 2 expands supersonically, and neither sound nor entropy waves can cross the ablation front and affect the flow in region 1. The assumption of  $\delta V_2 = 0$  may not be a unique boundary condition. As a matter of fact, we have obtained similar results as explained below even with the boundary condition of  $\delta T_2 = 0$ . Therefore, it should be possible to solve the problem in region 1, by choosing “plausible” boundary conditions at the sonic point.

We consider a rippled shock wave driven by an initial corrugated surface. The coefficients and the separation constant of Eq. (4) are determined by the initial and boundary conditions. The solution containing the Neuman function  $N_{\mu}$  must be dropped out to satisfy initial conditions at the ablation front ( $\delta I \equiv 0$ ). Moreover, the index  $\mu$  must be a positive odd integer to satisfy the initial and boundary conditions at the shock front [ $a_s(0) = a_a(0) = a_0$ ]. Therefore, Eq. (4) becomes  $\delta p_1 = \sum_{n \geq 0} \{E_n e^{-(2n+1)\theta} + F_n e^{+(2n+1)\theta}\} J_{2n+1}(r)$ , where the separation constant  $n$  is an integer, and the coefficients  $E_n$  and  $F_n$  are determined by the boundary conditions. We can also express  $a_s$  and

$a_s$  by using Eqs. (5) and (6), respectively.  $a_s$  and  $a_a$  are functions of  $r_s = kc_1t\sqrt{1 - [(u_s - v_{x1})/c_1]^2}$  and  $r_a = kc_1t\sqrt{1 - [(u_a - v_{x1})/c_1]^2}$  because the shock and ablation fronts propagate along the trajectories  $x = u_s t$  and  $x = u_a t$ , respectively.

Figure 2 shows the shock front ripple (solid line),  $a_s/a_0$ , as a function of  $r_s$  and the ablation surface deformation (dot-dashed line),  $a_a/a_0$ , as a function of  $r_a$ . The parameters used are  $I = 4 \times 10^{13}$  W/cm<sup>2</sup>,  $\lambda_L = 0.53$   $\mu$ m,  $\rho_0 = 1.06$ g/cm<sup>3</sup> (CH target),  $p_0 = 0.703$  Mbar (equivalent to  $T_0 = 1$  eV),  $\lambda = 100$   $\mu$ m,  $\gamma_0 = 3$ ,  $\gamma_1 = 3$ , and  $\gamma_2 = 5/3$ , where  $\lambda_L$  is laser wavelength. Once a rippled shock is launched, a pressure perturbation is induced by the lateral fluid motion behind the shock. The pressure perturbation causes the ripple of the shock front to be reversed and subsequently oscillate, as the pressure perturbation increases the deformation of the ablation front monotonously. The amplitude of the shock ripple decays as the shock propagates. Since the pressure perturbation at the ablation front also decays with time, the deformation of the ablation front approaches an asymptotic value as shown in Fig. 2. It takes longer time for the ablation surface deformation to reach the asymptotic value as compared with the oscillation period of the rippled shock. It should be also noted that the increase of the ablation surface deformation is different from the Richtmyer-Meshkov (RM) instability because in the RM instability there is a finite growth rate,  $\dot{a}_a \neq 0$ , and thus no asymptotic amplitude [8,11]. In comparison with the rippled shock driven by a rippled rigid piston (dotted line in Fig. 2) [7,9], the amplitude of the shock surface ripple driven by laser ablation decays much faster than that driven by the rigid piston. This is due to the fact that in the laser ablation case the pressure perturbation behind the shock is weakened because of the mass flow across the ab-

lation surface and also because of the deformation of the ablation surface that accompanies the perturbed pressure.

In the weak shock limit, it seems reasonable that the first terms ( $E_0$  and  $F_0$ ) are dominant in the solution for  $\delta p_1$  [11]. In addition, since the ablation Mach number is much smaller than unity [ $(u_a - v_{x1})/c_1 = v_a/c_1 \ll 1$ ], by expanding the coefficients into a power series of  $v_a/c_1$  and retaining the leading order term, we get:

$$\frac{a_s(t)}{a_0} \approx J_0(r_s) + \frac{2M_s^2 + 2}{3M_s^2 + 1} J_2(r_s). \quad (8)$$

This approximate formula is shown by circles in Fig. 2, which agrees quite well with the exact solution even for relatively large  $M_s (= 3.74)$ . On the other hand, the calculation of  $a_a(t)$  is not as straightforward as for  $a_s(t)$ . However, we can get an asymptotic value for  $a_a$ :

$$\frac{a_a(\infty)}{a_0} \approx 1 + \frac{8M_s^2(M_s^2 - 1)}{(3M_s^2 + 1)[2\gamma_1 M_s^2 - (\gamma_1 - 1)]} \frac{c_1}{v_a}. \quad (9)$$

The asymptotic value of the ablation surface deformation increases monotonously as the shock intensity increases. However, the exact solution starts to saturate around the shock intensity of  $(p_1 - p_0)/p_1 \sim 0.6$ . The shock intensity of 0.6 corresponds to the absorption intensity of  $\sim 10^{13}$  W/cm<sup>2</sup> for the parameters used, since in our model the shock intensity is determinate by the absorbed laser intensity through the CJ jump conditions.

In Fig. 3, we compare the theoretical values with the experimental results [5]. Figures 3(a) and 3(b) show the normalized shock front ripple,  $a_s/a_0$ , and the normalized perturbation of the areal mass density,  $\delta\rho l/(\delta\rho l)_0$ , respectively, as functions of the normalized time,  $u_s t/\lambda$ , where  $(\delta\rho l)_0$  is an initial value of the areal mass density perturbation. The parameters used are the same as those in Fig. 2. Both the oscillation period and decay rate of the rippled shock front agree quite well with the experimental results as shown in Fig. 3(a). In Fig. 3(b), agreement between the theory and the experiment is also found on the areal mass density perturbation.

We now also investigate a rippled shock driven by nonuniform laser irradiation on a smooth target. We can determine the coefficients and separation constant of Eq. (4) by using the boundary conditions and the initial conditions given by  $a_s(0) = a_a(0) = 0$  and  $\delta I \equiv \text{const}$ . As a result, Eq. (4) becomes  $\delta p_1 = \sum_{n \geq 0} \{E_n e^{-2n\theta} + F_n e^{+2n\theta}\} J_{2n}(r)$ . In this problem, since the nonuniformity is continuously supplied by laser, there is a finite asymptotic value of the velocity perturbation of the ablation front contrary to the previous case. In the weak shock limit, we can obtain the approximate formulas for both the shock front ripple,  $a_s(t)$ , and the asymptotic growth rate of the ablation surface,  $\dot{a}_a(\infty)$ :

$$\frac{ka_s(t)}{\delta I/I} \approx K_1 \left[ J_1(r_s) + \frac{(2 - \beta_s^2)M_s^2 + 3}{(2 + \beta_s^2)M_s^2 + 1} J_3(r_s) \right], \quad (10)$$

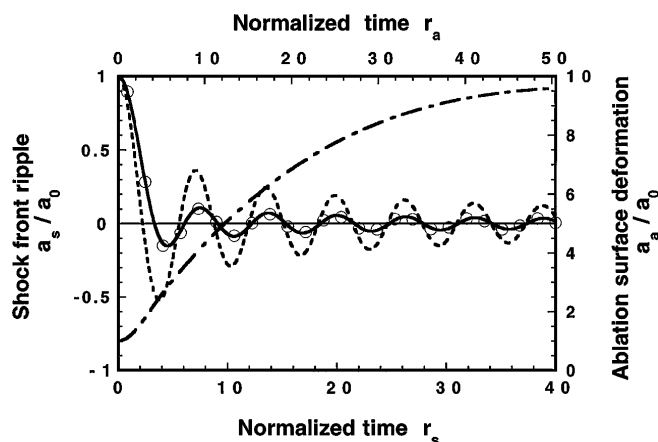


FIG. 2. Shock front ripple,  $a_s/a_0$ , and ablation surface deformation,  $a_a/a_0$ , as functions of normalized times  $r_s$  and  $r_a$ , respectively. Solid line and circles show the exact solution and approximate formula of  $a_s/a_0$ , respectively. A dotted line shows  $a_s/a_0$  driven by a rippled piston. Dot-dashed line shows the exact solution of  $a_a/a_0$ .

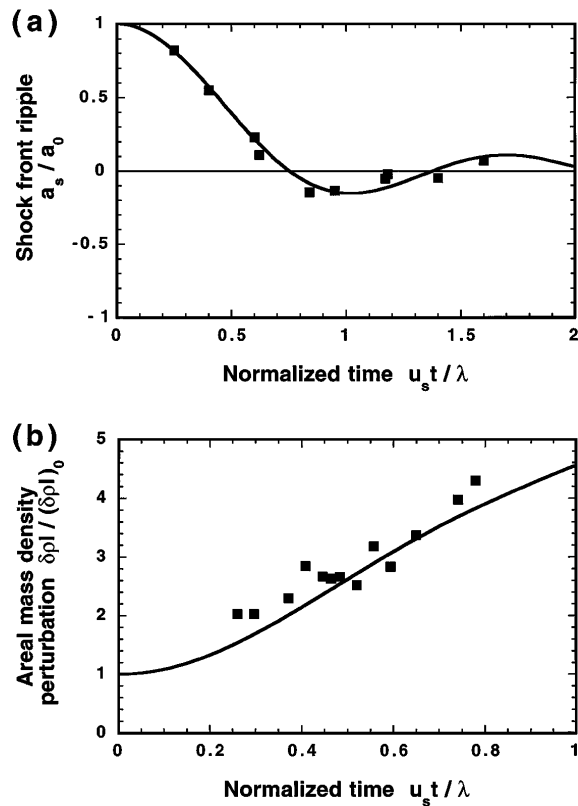


FIG. 3. (a) Shock front ripple,  $a_s/a_0$ , and (b) areal mass density perturbation,  $\delta\rho l/(\delta\rho l)_0$ , as functions of normalized time,  $u_s t/\lambda$ . Solid lines are theoretical values, and squares experimental results.

$$\frac{\dot{a}_a(\infty)/c_1}{\delta I/I} \approx \frac{2}{3\gamma_1} \frac{c_1}{v_a} \left[ 1 + K_2 \frac{M_s^2 - 1}{(2\beta_s^2 + 1)M_s^2 + 1} \right], \tag{11}$$

where  $\beta_s$  is the shock Mach number with respect to the fluid behind the shock,  $K_1 = (\gamma_1 + 1)/[3\gamma_1\beta_s\sqrt{1 - \beta_s^2}]$ , and  $K_2 = (1 - \beta_s)/(1 + \beta_s)$ . In Fig. 4, we compare the results of Eqs. (10) and (11) with the exact solutions. Figure 4 shows the normalized shock front ripple,  $ka_s/(\delta I/I)$ , as a function of  $r_s$  and the normalized growth rate of the ablation surface,  $(\dot{a}_a/c_1)/(\delta I/I)$ , as a function of  $r_a$ . The parameters used are the same as those of the previous problem. Since the higher laser intensity drives the larger ablation pressure, the shock front ripple increases with time at first and oscillates subsequently. The first maximum of the dimensionless shock ripple reaches  $\sim 0.65$  for the parameters used. The asymptotic value of  $\dot{a}_a$  has a weak dependence of the shock intensity. Namely,  $(\dot{a}_a/c_1)/(\delta I/I)$  is  $\sim 5-7$  for low to high shock intensity [ $0 < (p_1 - p_0)/p_1 < 1$ ]. We have also found a good agreement between the approximate formulas given by Eqs. (10) and (11) and the exact solutions for a wide range of the shock intensity.

We have developed a simple analytical model to investigate propagation of a rippled shock driven by nonuni-

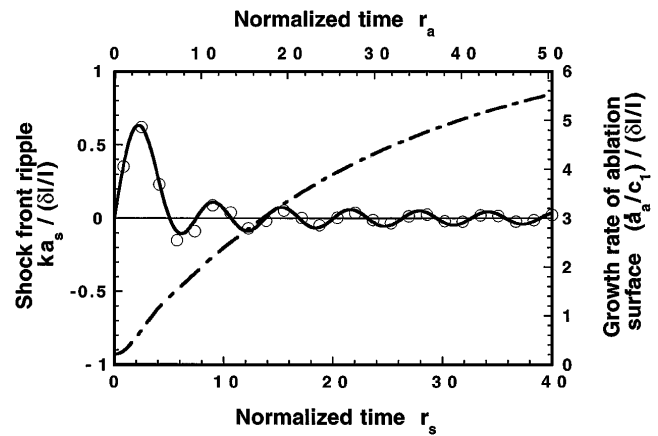


FIG. 4. Shock front ripple,  $ka_s/(\delta I/I)$ , and growth rate of ablation surface,  $(\dot{a}_a/c_1)/(\delta I/I)$ , as functions of normalized times  $r_s$  and  $r_a$ , respectively. Solid line and circles show the exact solution and approximate formula of  $ka_s/(\delta I/I)$ , respectively. Dot-dashed line shows the exact solution of  $(\dot{a}_a/c_1)/(\delta I/I)$ .

form laser ablation induced by an initial surface roughness of a target or nonuniform laser irradiation on a smooth target. In the weak shock limit, we obtain approximate formulas for the shock front ripple and the asymptotic behavior of the ablation surface.

We are grateful to Dr. J. G. Wouchuk for valuable suggestions relating the asymptotic formulas. We thank Mr. K. Shigemori, Professor H. Azechi, and Professor K. Mima for many useful discussions.

---

[1] J. Nuckolls *et al.*, *Nature (London)* **239**, 139 (1972).  
 [2] S. Chandrasekhar, *Hydrodynamic and Hydromagnetic Stability* (Oxford Univ. Press, London, 1968), Chap. 10.  
 [3] H. Takabe *et al.*, *Phys. Fluids* **28**, 3676 (1985); J. Grun *et al.*, *Phys. Rev. Lett.* **58**, 2672 (1987); B. Remington *et al.*, *Phys. Rev. Lett.* **67**, 3259 (1991).  
 [4] I. Hachisu *et al.*, *Astrophys. J.* **390**, 230 (1992).  
 [5] T. Endo *et al.*, *Phys. Rev. Lett.* **74**, 3608 (1995).  
 [6] P. M. Zaidel, *J. Appl. Math. Mech.* **24**, 316 (1960).  
 [7] M. G. Briscoe and A. A. Kovitz, *J. Fluid Mech.* **31**, 529 (1968).  
 [8] R. D. Richtmyer, *Commun. Pure Appl. Math.* **13**, 297 (1960).  
 [9] R. Ishizaki *et al.*, *Phys. Rev. E* **53**, 5592 (1996).  
 [10] H. Takabe *et al.*, *J. Phys. Soc. Jpn.* **45**, 2001 (1978).  
 [11] J. G. Wouchuk and K. Nishihara, *Phys. Plasmas* **3**, 3761 (1996).  
 [12] R. J. Taylor *et al.*, *Phys. Rev. Lett.* **76**, 1643 (1996); D. H. Kalantar *et al.*, *Phys. Rev. Lett.* **76**, 3574 (1996).  
 [13] W. M. Manheimer, and D. G. Colombant, *Phys. Fluids* **27**, 983 (1984).  
 [14] J. G. Wouchuk and A. R. Piriz, *Phys. Plasmas* **2**, 493 (1995).